Biochimica et Biophysica Acta 903 (1987) 292–302
Elsevier

BBA 73688

The transport of hydrophobic ions across lipid bilayers

H.P. Braun

Institut für Physikalische und Theoretische Chemie der Technischen Universität München, Garching (F.R.G.)

(Received 18 May 1987)

Key words: Hydrophobic ion; Lipid bilayer; Membrane capacitance; Ion transport

The three-capacitor model for hydrophobic ion adsorption in lipid membranes (Andersen, O.S., Feldberg, S., Nakadomari, H., Levy, S. and McLaughlin, S. (1978) Biophys. J. 21, 35–70) is extended to ion transport whereby electrostatic effects from the interfacially adsorbed hydrophobic space charge have been encountered. The phenomena of current saturation with increasing concentrations of hydrophobic ions in the bulk electrolyte and the associated increase of the time constant of current relaxation can be quantitatively understood on the basis of space charge-limited currents as well as the nonexponential current decay.

Introduction

The permeation of lipid-soluble (hydrophobic) ions through artificial lipid bilayers is referred to, in some aspects, as a model system for ion transport in biological membranes [2]. The effect of hydrophobic ion conduction is observed as a transient current upon the application of a voltage, in the presence of hydrophobic ions in the electrolyte surrounding the membrane. Theories have been developed mainly on the basis of electro-diffusion [3–6] and an Eyring rate theory model [7].

At high concentrations of hydrophobic ions in the bulk electrolyte, however, some experimental observations are difficult to interpret along the lines of the current theories: The initial current saturates or even decreases with increasing concentration of hydrophobic ions; simultaneously, the time course of current decay becomes nonexponential and the time constant rises [1,7–10]. In view of the model character for the ion transport, the differences should be explained by an understanding of the interrelationship between the observables, assumed to be independent so far.

In contrast to the dynamic properties of current transport, the electrostatic properties of ion adsorption into the membrane are well understood. The potential energy curve for a hydrophobic ion in the membrane shows absolute minima close to the electrolyte interfaces, where the ions adsorb. The spatial confinement of the accumulated charge as on a parallel plate capacitor justifies the use of capacitors as equivalent circuit elements for a membrane [1]. In the present article a further consequence of the energy curve is discussed, concerning different energetic states of the hydrophobic ions. Ions in the adsorbed state are assumed to be in equilibrium with desorbed ions. The adsorbed ones are thought to be immobile, not contributing to the current, though they will add to the static electric field. Bruner [8] and Andersen et al. [1] have determined the amount of hydrophobic charge adsorbed at the interfaces of a membrane. Charge densities of the order of 1 $\mu C/cm^2$ of membrane area were found for high ion concentrations in the aqueous electrolyte. Such a charge density would generate an electric field,

---

Correspondence: H.P. Braun, Institut für Physikalische und Theoretische Chemie der Technischen Universität München, Lichtenbergstrasse 4, D-8046 Garching, F.R.G.

0005-2736/87/$03.50

$E = q^0/\varepsilon$, of 10^6 V/cm corresponding to a potential of 1 V applied to a membrane of 5 nm thickness. The influence of the adsorbed charge on the kinetics of ion transport is discussed in this article.

Theoretical background

The three-capacitor model [1,14] presents a simple picture of the spatial distribution of hydrophobic charges in a membrane. It is based on the commonly accepted assumption that hydrophobic ions adsorb into minima of the potential energy [4,5,7,15], forming thin layers of charge within the membrane close to the electrolyte interfaces. Three regions of membrane dielectric are separated by the resulting two planes of adsorbed charges. Fig. 1(d) shows the geometry of the three-capacitor model. Each region is considered as a parallel plate capacitor. The 'plates' of the inner capacitor, C_i, are formed by the accumulation layers of hydrophobic ions, extending for a distance, l_a, from the physical border into the membrane. The capacitor is filled with a dielectric of low dielectricity constant, namely, the hydrocarbon chains of the lipid molecules. The interfacial capacitors, C_o, each of them sharing one plate with the inner capacitor, extend across the lipid/electrolyte interface. According to the Gouy-Chapman theory, it is assumed that the counter ions of the hydrophobic salt concentrate in the electrolyte are about one Debye length, l_D, away from the membrane surface. Its center of charge designates the location of the outer plate of C_o. The dielectric material within C_o consists of the polar head groups of the lipid and of water molecules from the electrolyte. These three capacitors connected in series make up the membrane capacitance, C_m, which is measured externally.

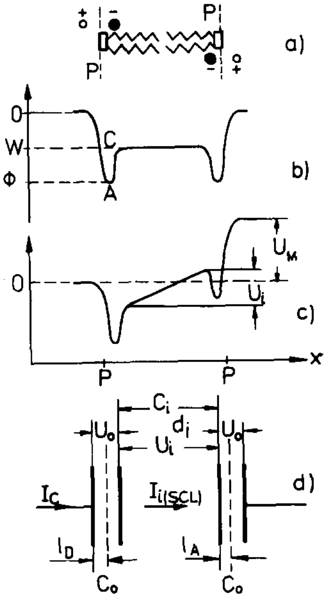

Fig. 1. (a) Geometry of the three-capacitor model. P, physical borders of the membrane, zig-zag line indicates hydrocarbon chains of the lipid molecules; filled black circles, location of the adsorbed hydrophobic ion; open circle, location of the co-ions in the electrolyte. (b) Total membrane potential for a hydrophobic ion in a lipid membrane in thermal equilibrium. ϕ, micropotential of the adsorption layer with respect to the bulk electrolyte $\phi = 0$; W, hydrophobic barrier; A, adsorbed state; C, conducting state of the hydrophobic ions. (c) Potential immediately after the application of an external voltage U_M. U_i, voltage drop across the inner capacitor. (d) Equivalent circuit. C_o, interfacial capacitor with total spacing $l_a + l_D$; l_D, distance of the co-ions from the physical border of the membrane, equal to the Debye screening length in the aqueous electrolyte; l_a, distance of the accumulation layer from the physical border of the membrane; C_i, inner capacitor; $U_{o,i}$, voltage drop of the external potential, U_M, across the individual capacitors; I_i, current flowing in the inner capacitor; I_c, externally measured current.

After the derivation of the principal current-voltage relationship for the inner capacitor the influence of the adsorbed charge, q^0, on the current-voltage curve will be examined. Finally, we account for the three-layered structure and introduce corrections for the coupling of the current via the interfacial capacitors.

The role of the total potential energy curve for the energetical and spatial distribution of hydrophobic ions

With the calculation of the potential energy of a hydrophobic ion in a lipid membrane [4,5,7,12], the effect of interfacial ion accumulation becomes comprehensible: A superposition of dielectric, hydrophobic and image forces repels the hydrophobic ions from the interior of the membrane and attracts them towards deep potential minima close to the interfaces of the membrane, where they adsorb. Both layers of adsorbate are separated by an energy barrier constituted of the hydrocarbon chains in the middle of the membrane. By adsorption to the polar region of the membrane, the hydrophobic ions occupy the absolute minimum state of their potential energy. Commonly, the adsorbed charge, q^0, as a function of the ion concentration in the bulk electrolyte, c_{aqu} is described by Eqn. 1 [1,7,13,14]

$$q^0 = ne = eMAc_{\mathrm{aqu}} \exp -((e\phi + \gamma(n/m))/kT) \tag{1}$$

where e is the unit charge, M the number of adsorption sites per area A, ϕ the micropotential measured relative to the bulk electrolyte and kT the thermal energy. γ accounts for an energetical spread of the ions due to their lateral interaction in the adsorption layer [14]. This charge is fixed or adsorbed and cannot contribute to the current. In thermal equilibrium only a fraction, θ, of the adsorbed charge q^0 has sufficient energy to escape from the potential dip and reach a level, W, from where the ions can be drifted across the interior of the membrane by an external field. The mobile charge, q_{m}, at the emitter side (location C in Fig. 1(b)) is approximately given by the Boltzmann factor:

$$q_{\mathrm{m}} = q^0 \exp((W - \phi - \gamma(n/M))/kT) = q^0\theta \tag{2}$$

The voltage drop of the external potential across l_{a} is assumed to be much less than $(\phi - W)$ so that it will not influence θ. $(\phi - W)$ can be interpreted as an activation barrier for the transition from the adsorbed into the conducting state. Indications for the existence of mobile and immobile charges in a lipid membrane were found by Wulf et al. [10]. They have optically determined the concentration of adsorbed hydrophobic ions, which turned out to be larger than the mobile hydrophobic charge being probed by current measurements. It is concluded that not all adsorbed ions contribute to the electrical conductance [15].

The current voltage curve for the membrane is derived by combining the Poisson equation

$$\mathrm{d}F/\mathrm{d}x = q^0(x)/\varepsilon \tag{3}$$

with the equation for the drift current, neglecting the diffusive current

$$I = A\mu q_{\mathrm{m}}(x)F(x) \tag{4}$$

yielding a differential equation for the electric field $F(x)$ [16–20]. For mathematical details, see Appendix A. The layer of adsorbed charge in front of the emitter screens a part of the external potential, which is accounted for by the screening factor, S_{e}, (see Appendix B), thus obtaining for the current-voltage curve

$$I_{\mathrm{SCL}} = (9/8)S_{\mathrm{e}}A\varepsilon\mu U_{\mathrm{i}}^2/d_{\mathrm{i}}^3 \tag{5}$$

We will arrange Eqn. 5 in a form which refers to the capacitor equivalent of the membrane.

$$I_{\mathrm{SCL}} = (9/8)(\varepsilon AU_{\mathrm{i}}/d_{\mathrm{i}})(S_{\mathrm{e}}\mu U_{\mathrm{i}}/d_{\mathrm{i}}^2) \tag{6}$$

The second factor denotes the capacitance, C_{i}, multiplied by the voltage U_{i}, being equal to the charge Q, to which the inner capacitor is charged. The third term is equal to the reciprocal of the transit time, t_{o}, which the ions need to drift across the spacing d_{i}.

Approximating the first factor by 1, we reformulate Eqn. 6 by

$$I_{\mathrm{SCL}} = Q/t_{\mathrm{o}} \tag{7}$$

It is a property of the space charge-limited conduction in membranes that the applied voltage places a charge Q for translocation at the emitting layer, which corresponds exactly to the capacitor equation $Q = C_{\mathrm{i}}U_{\mathrm{i}}$. Thus, the square law dependence on the voltage in Eqn. 6 is due to the fact that the amount of transferable charge on the membrane capacitor and the ion velocity both increase linearly with voltage. These two laws are sufficient to describe the conduction of hydrophobic ions in lipid membranes!

Another characteristic of this current voltage relationship is the current decrease with the third power of the membrane spacing. Space charge-limited currents can be easily separated from other conduction mechanisms by examining both the voltage and thickness dependence.

The influence of the adsorbed charge on the kinetics of ion transport

From the third factor of Eqn. 6, one can formally define an effective mobility, μS_{e}, resulting from the partially screened external potential. This will explain the observation of a slower time constant t_o for current relaxation in the saturation regime.

$$t_o = d_i^2/(\mu S_e U_i) \tag{8}$$

We see that the apparent decrease in ionic mobility or membrane fluidity [8] can also be explained by electrostatic effects. The current reduction by fixed charges has been extensively studied in solid-state electronics [16–22] and detailed mathematical derivations for the present geometry are given in Refs. 18–22.

The observation of the transient current is easily understood on the basis of the potential curve of Fig. 1(b). Since the translocated ions cannot leave the inner capacitor, they will compensate for the external voltage with a counter potential generated by their own charges. Current flow will stop either when the external potential is totally compensated by the internal potential of the translocated ions or when the interfacial layer can no longer supply charges for translocation. We focus on the first condition and express Eqn. 7 by the integral relationship

$$Q = I_{\mathrm{SCL}} \int_0^{\infty} f(t)\,\mathrm{d}t = I_{\mathrm{SCL}} t_o \tag{9}$$

where $f(t)$ is the 'decay function' of the current obeying the boundary conditions $f(0) = 1$ and $f(t_\infty) = 0$. The integral over $f(t)$ justifies the use of the transit time t_0 (Eqn. 8), as a characteristic time constant for the transport of the whole charge Q across C_i. Inserting the quadratic current-voltage dependence of Eqn. 5 into Eqn. 9, we find for the time course of the current (see Appendix C)

$$I_{\mathrm{SCL}}(t) = I_{\mathrm{SCL}}(1 + t/t_o)^{-2} \tag{10}$$

Eqn. 7 provides a simple criterion to distinguish the conduction regime of the membrane by comparing the mobile charge to the translocated charge

$$\theta q^0 < Q \tag{11a}$$

$$\theta q^0 \geqslant Q \tag{11b}$$

Eqn. 11a represents the case where less mobile charge is concentrated in the layers than the capacitor can hold at the applied voltage. Consequently, the translocated charge is no longer voltage dependent. Only the ion velocity will increase with voltage and a linear current-voltage relationship will result. In order to calculate the concentration dependence, we use Eqns. 1 and 2, which relate the adsorbed and the mobile charge to the hydrophobic ion concentration in the bulk electrolyte. We obtain the linear dependence for the low concentration case [2].

$$I = \theta q^0 \cdot \mu U_i / d_i^2 \tag{12}$$

Fig. 2 shows the initial current at constant voltage, plotted against the aqueous concentration of the hydrophobic salt. Eqns. 11a and 12 define the well-known constant conductivity at low ion concentrations, as illustrated by curve A. When the mobile charge at the interfaces exceeds the charge Q on the capacitor, the transferable charge is now limited by the fixed voltage of the inner capacitor (see Eqn. 7). A further increase of mobile ions at the interfaces has no influence upon the charge Q on the capacitor. Consequently, the current saturates with increasing concentration of hydrophobic ions. This is the fundamental idea of space charge limitation, which explains the observed saturating current. The horizontal dashed line (B) in Fig. 2 illustrates the current saturation in the space charge-limited regime. In the present model we find the origin of current saturation in the finite charging capability of the inner mem-

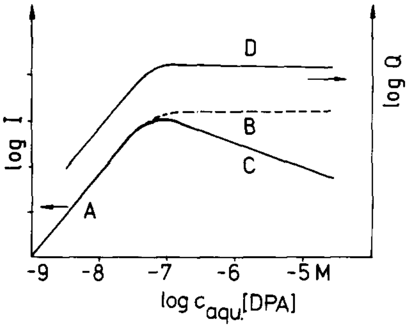

Fig. 2. Schematic representation of the initial membrane current at constant voltage versus concentration of hydrophobic ions in the aqueous electrolyte. Curve A, linear regime; B, ideal space charge-limited current; C, interface charge-limited current with which the ratio of mobile to adsorbed charge decreases with the concentration of hydrophobic ions; D, amount of translocated charge, Q.

brane capacitor for a given voltage. The equality of θq^0 with the transferable charge Q (Eqn. 11b) defines the space charge regime. Though the transferable charge is insensitive to a further increase of the adsorbed charge, the ratio of adsorbed to free ions will still influence the kinetics of current transport. With increasing concentration of hydrophobic ions the micropotential will rise with the number of adsorbed ions, due to their electrostatic interaction in the accumulation layer. Eqn. 2 then predicts a decreasing ratio of free to adsorbed ions. This change in θ becomes observable via the screening factor S_e in the reduced current (curve C) and in the increased time constant for the current relaxation.

Completion of the three-capacitor model

We now turn to the last point in the adaptation of the three-capacitor model and investigate the coupling of the inner current, I_{SCL}, to the external current, I_c, via the interfacial capacitors. They were assumed to exchange hydrophobic ions on a much slower time scale than the inner capacitor. Therefore, the current, I_{SCL}, which is measured in the external circuit is somewhat less than the current flowing in the central part of the membrane because the charge is physically displaced across C_i, whereas the external potential is applied across the three capacitors in series. Andersen et al. [1] and Feldberg and Delgado [26] have calculated this correction factor, which is similar to that of a capacitive voltage divider.

$$I_c = I_{SCL} C_m / C_i \tag{13}$$

The ratio of the capacitances is always close to unity [26]

Experimental details

Sample preparation

Black lipid films were prepared according to the technique of Mueller et al. [27]. The lipid used was a solution of dioleoylphosphatidylcholine 18:1 (Sigma) in *n*-alkanes at a concentration of 2% (w/v). The unbuffered aqueous electrolyte consisted of a 0.1 M solution of sodium chloride (Merck) in distilled water. The temperature of the electrolyte was 21° C. A membrane prepared with *n*-decane under these conditions will be referred to as a 'standard' membrane. Dipicrylamine, supplied by Fluka AG, was added to the aqueous electrolyte. The average thickness of the membrane was varied by the amount of alkane solvent being incorporated. The smaller the molecule the larger is its solubility in the membrane [28]. *n*-Octane, decane, dodecane and hexadecane (Fluka, puriss.) were used as solvents. The thickness of the lipid film was determined from its capacitance, assuming a relative dielectric constant of 2.1 [28]. The electric circuit for charging the bilayer consisted of a triggerable pulse generator with 50 Ω ouput impedance, providing a bipolar voltage pulse with independent amplitude and pulse length settings for each polarity. The current was measured using a current to voltage converter with a sensitivity of 1 $\mathrm{V}/10^{-7}$ A, an effective input resistance of 1 kΩ and a bandwidth of 50 kHz. Ag/AgCl electrodes with an area of 3 cm^2 were used, giving a path resistance in the electrolyte of 300 Ω with 0.1 m NaCl. Processing of the current signal was performed by a digital averager with a resolution of 13 bit on the vertical axis and 20 μs per point on the time axis. For details see Ref. 29. For the most part, ten measurements per voltage setting were averaged. The data on the concentration dependence represent averages over nine different membranes.

Comparison of space charge-limited current predictions with experiments

Numerous data have been published concerning the current-voltage relationship for various lipids and hydrophobic ions. In the following we reinvestigate some of these data, together with own results, in the light of the SCLC theory. The dependence of the initial current upon the square of the applied voltage is depicted in Fig. 3 for hydrophobic ions of both polarities. The current-voltage relationship we observe for standard membranes with $5 \cdot 10^{-7}$ M dipicrylamine is shown in curve a. The influence of the diffusion current on the current-voltage curve has been tested by preparing a standard membrane with asymmetric dipicrylamine concentrations of 10^{-7} and 10^{-6} M. The current voltage curves (b) are still quadratic, and the stationary diffusive current for zero exter-

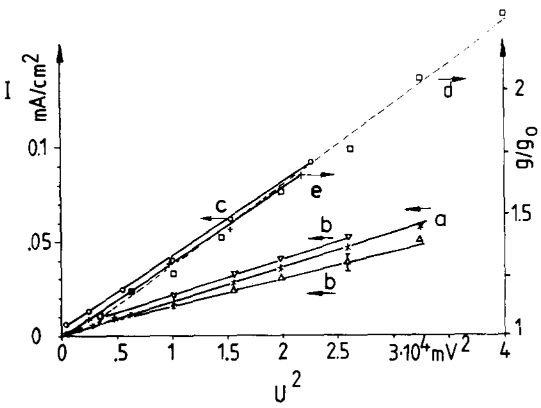

Fig. 3. Initial current as a function of the square of the applied voltage. (a) Current voltage curve for a standard membrane with $5 \cdot 10^{-8}$ M dipicrylamine. (b) Standard membrane in asymmetric electrolytes of 10^{-7} and 10^{-6} M dipicrylamine? (multiply current scale by 10 for (a) and (b)). (c) Circles indicate experimental data taken from Table 2 of Ref. 30. The membrane was formed from a cholesterol/monolein mixture (5 : 1) in an aqueous solution of 0.1 M NaCl with $2 \cdot 10^{-7}$ M tetraphenylborate. The initial current was measured under a constant biasing potential of −100 mV. (d) Replot in units of small field conductivity g_0 for a membrane of bacterial phosphatidylethanolamine in decane with $7 \cdot 10^{-8}$ M tetraphenylborate in 0.1 M NaCl. Data are taken from Fig. 11 in Ref. 5. (e) is normalized to the conductivity at 10 mV. A glycerol monooleate membrane in *n*-hexanedecane in a 10^{-4} M solution of tetraphenylarsonium was used. Experimental data originate from Fig. 1 in Ref. 31.

nal potential is negligible when compared to the drift current at low voltages (25 mV). The upper curve is for negative polarity of the compartment containing the 10^{-7} M concentration and the lower curve is for positive polarity. Curve c is a plot of data for tetraphenylborate in oxidized cholesterol films given in Table 2 of Ref. 30. The experimental points of curve d were taken from Fig. 11 of Ref. 5, a bacterial phosphatidylamine membrane with $7 \cdot 10^{-8}$ M tetraphenylborate and curve e is a current-voltage curve for positively charged hydrophobic ions taken from Fig. 1 in Ref. 31. All available data of initial currents exhibit this square law relationship. At very high voltages (0.2–0.4 V), linear current-voltage curves are reported (e.g., Fig. 1 of Ref. 8). Charging the membrane capacitor at high voltages requires a large Q which can exceed the adsorbed charge, q^0, Eqn. 11a then applies with the appropriate conclusions given there.

Another characteristic of space charge-limited currents is their dependence on the inverse third power of the membrane thickness. Curve a in Fig. 4 shows the initial current of the lipid membrane for different average thicknesses, due to varying amounts of incorporated solvent. A concentration of $1 \cdot 10^{-8}$ M dipicrylamine was used throughout the experiments and the exciting voltage pulse was 50 mV. Curves b and c are taken from Fig. 1 in Ref. 32.

Space charge-limited current prediction and experiment agree remarkably well. Fig. 5 illustrates hwo the initial current (5(a)) and the time constant of current relaxation (5(b)) depend upon the concentration of hydrophobic ions in the electrolyte. The translocated charge Q calculated from Fig. 5 is shown in Fig. 6(a). We find a constant amount of translocated charge Q, clearly indicating the existence of space charge-limited currents in lipid membranes. The observation of a constant charge Q for dipicrylamine in phosphatidylcholine films was also reported by Bruner (Fig. 10 in Ref. 8) and by Wulf et al. [10], and for tetraphenylborate it can be verified by calculating the transferred charge from Figs. 3 and 4 of Ref.

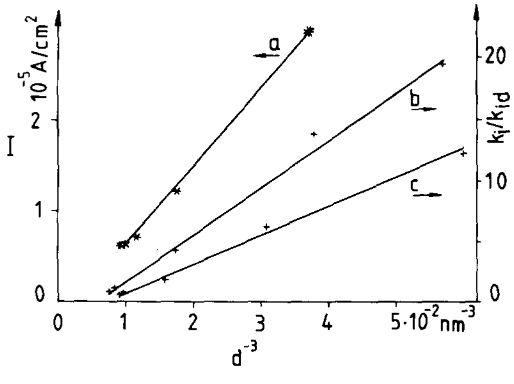

Fig. 4. Initial current as a function of the membrane thickness. The thicknesses of the membranes were varied by changing the content of alcane solvents. Solvents with low molecular weight are better incorporated into the membrane than heavier ones [28,32]. (a) Membrane of standard preparation, with $5 \cdot 10^{-7}$ M dipicrylamine, measured at 50 mV. The data of (b) and (c) were taken from Fig. 1 in Ref. 32. The transport rates are normalized to the rate k_D of a membrane prepared with *n*-decane as solvent. Curve (b) is for a dioleoylphosphatidylcholine membrane with 10^{-8} M dipicrylamine and (C) is for monoolein with $3 \cdot 10^{-8}$ M dipicrylamine (multiply horizontal scale by 10).

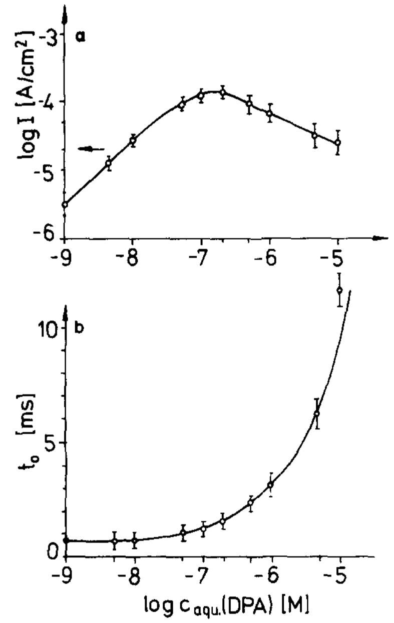

Fig. 5. (a) Initial current at constant voltage (50 mV) for a membrane with a standard preparation as a function of dipicrylamine (DPA) concentration in the aqueous electrolyte (solid curve). (b) Time constant for the relaxation of the initial current of Fig. 5(a). The time constant, τ_0, of the linear regime has been determined on the basis of an exponential decay, the time constant, t_0, in the space charge-limited regime is determined according to Eqn. 10.

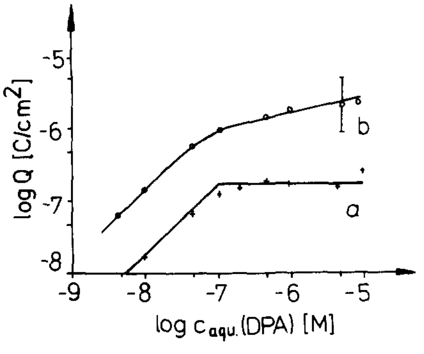

Fig. 6. (a) Mobile, hydrophobic charge, Q, transported by the current (product of I from Fig. 5(a) and t_0 from Fig. 5(b)). (b) Hydrophobic charge adsorbed into a standard membrane, determined by the application of high-voltage pulses, similar to Ref. 8. DPA, dipicrylamine.

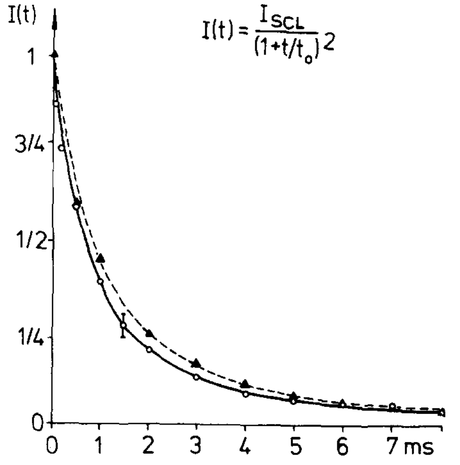

Fig. 7. Time course of current decay. Solid curve is calculated according to Eqn. 10, with a time constant of 1.7 ms for a standard membrane with $5\cdot 10^{-7}$ M dipicrylamine and 10^{-2} M NaCl after applying a voltage pulse of 50 mV. The initial current was $1.8\cdot 10^{-4}$ A/cm². The stationary current for long times is subtracted. Data for the dashed curve were taken from Fig. 8 of Ref. 1 for a membrane of bacterial phosphatidylethanolamine where the current decay has been measured under a voltage of 160 mV.

1. Fig. 7 illustrates the hyperbolic time dependence of the current decay. $I(t)$ is fitted to a $(1 + t/t_0)^{-2}$ hyperbola. The solid curve is for a standard membrane with $5 \cdot 10^{-7}$ M dipicrylamine. The dashed curve is a replot of Fig. 8 in Ref. 1. The hyperbolic time law holds for the entire time range.

Discussion

The present approach shows that space charge effects are a consequence of the double minimum potential for hydrophobic ions with respect to their spatial location and energy distribution. An important feature of the potential curve can be seen in confining the ion transport to the volume between the accumulation layers, thus restricting the exchange of ions with the bulk electrolyte. Therefore, the layers are kinetically insulated from the surrounding electrolyte, which is unable to supply or drain ions on a time scale which is faster or comparable to the inner ion transport. Several important consequences for the transient current arise from this kinetic insulation:

(a) Since the interfacial layers are not in thermal equilibrium with the surrounding electrolyte, we use Poisson's law instead of Boltzmann's law to express the relationship of the charges on the interfacial layers and the electric potential generated between them. The volume enclosed by the accumulation layers then behaves as a parallel plate capacitor and the charge being placed at the emitter is proportional to the external potential.

(b) The hydrophobic charge being placed onto the emitting layer can only enter the membrane when the electric field in the vicinity of the emitter is maintained for a period of the order of the transit time. This requires that the dielectric relaxation time of the charges being present in the membrane in thermal equilibrium is longer than the transit time. Charge equilibration in the membrane involves the considerably slower desorption kinetics across the interfacial layer, ranging in the 100 ms to second range, or even slower [15]. Thus, diffusion cannot play the dominant role in the transient current. In order to decide whether diffusion can be neglected, experiments were carried out where a concentration gradient of hydrophobic ions was maintained across the membrane. Experimental reality showed that an additional diffusive current leads neither to a deviation of the square law characteristic nor to a significant change in the magnitude of the transient current. The current voltage curves are simply shifted by a diffusion potential but behave in a similar way, as if the current voltage curve has been measured with a constant biasing voltage. The negligible influence of the diffusive current is due to the fact that a pure lipid membrane is an insulator, which does not supply ions from its own volume. All the ions in a membrane are of extrinsic origin from the surrounding electrolyte, and no charges are present in the interior of the membrane. In solid-state electronics the lack of an intrinsic current is considered as a sufficient criterion for the neglect of diffusive currents [25].

(c) The peculiar shape of the total potential curve gives rise to the coexistence of bound and mobile hydrophobic ions in the membrane interface. Ions residing in the absolute minimum of the potential curve will be considered as quasi-immobile, unable to contribute to the current. They are in equilibrium with free ions, which can be transferred by an external electric field. A change in the surface potential will be reflected by a changing ratio of adsorbed and mobile ions. Similar relationships to Eqn. 12 describing the ionic conductivity as a function of the surface potential are well established for lipid membranes. See, for example, Ref. 2 and references given therein. The present approach also includes the electrostatic screening by the adsorbed ions.

(d) The occurrence of internal polarisation at the collecting interface is a further consequence of the limited exchange of the ions with the surrounding electrolyte. Therefore, the translocated charge piles up in front of the collector and ion kinetics is governed by the difference of external and counter potential, leading to the hyperbolic decay in the transport velocity. The polarisation effect allows for the observation of a transient current which carries exactly the charge being injected into the membrane capacitor by the applied voltage.

(e) The non-exponential characteristic of the current decay appearing together with the phenomenon of current saturation is a result of the space charge-limited conduction. A pure exponential decay curve will always occur when the current is proportional to the applied voltage, i.e., when the current arises from a constant conductivity. Then, the observed time constant is simply the 'RC product' of the inner capacitor and its equivalent resistor for ion conduction. This condition is only met in the constant conductivity regime (Eqn. 11a). With the transition to the non-linear space charge-limited current, the hyperbolic time course is observed instead of the exponential one.

The idea of space charge-limited conduction in lipid membranes was first brought into discussion by O. LeBlanc in 1969 [33] explaining current saturation with space charge effects. Unfortunately, the shape of the total ion potential with the consequences of interfacial charge accumulation and subsequent screening was unknown at that time. 2 years later, in 1971, Ketterer et al. [7] mentioned the existence of accumulation layers. They described the ion transport by an Eyring transition state model, disregarding electrostatic effects. However, this formalism resulting in a voltage-dependent translocation rate does not account for the 2-fold action of the voltage on the ion velocity and on the injected charge, both being proportional to the voltage.

Space charge effects were predominantly investigated in electron- and hole-carrying devices

[11–25]. An exact solution for the equations of space charge limited-currents, including the diffusive current, has not yet been found. Recently, a series of publications appeared [11,12] which are also applicable for lipid membranes. Current flow in the presence of interfacially trapped charges is investigated in a geometry similar to ours. Solutions were given for the diffusion and drift dominated transport, respectively. At voltages smaller than the thermal voltage kT/e the diffusive current is dominant and a linear current voltage curve should result, even when space charge conditions prevail [21,22]. Experimental data, however, show a quadratic space charge characteristic, even down to a few millivolts. With this result it may be concluded that diffusion can be neglected.

Conclusions

It is demonstrated that space charge effects are a consequence of the total membrane potential for hydrophobic ions. The ratio of adsorbed versus mobile charge governs the kinetics of hydrophobic ion transport. All available experimental observations of the initial current in membranes doped with hydrophobic ions can be satisfyingly described within the simple picture of space charge limited-currents. Included are the voltage and thickness dependence, as well as the saturation phenomenon with increasing concentration of hydrophobic ions in the aqueous electrolyte and the non-exponential current decay. The relationship between the transient current and its time constant, hitherto considered as independent observables, is revealed. Current saturation is identified as a space charge effect. The translocated charge, measured by the product of the initial current and its decay time is constant in the saturation regime. The ratio of mobile to adsorbed charge turns out to decrease with increasing ion concentration, resulting in a decreasing current with an increasing time constant. The adsorbed charge in the accumulation layers, which is not involved in the ion transport, partially screens the external potential experienced by the mobile ions. The present observations favour a model for the transport of hydrophobic ions in lipid membranes, in which drift is dominant, rather than diffusion. An apparent similarity between the electron or hole injection into insulators and the transport of hydrophobic ions in membranes is noted.

Acknowledgements

The author wishes to thank Professor M.E. Michel-Beyerle and W. Lersch for many helpful discussions and Pauline Volk for the preparation of this manuscript. Financial support by J.A. and R. Braun and from the Deutsche Forschungsgemeinschaft is gratefully acknowledged.

Appendix A

Solution of the transport equations

The following equations were derived under the generally accepted assumption that the macroscopic laws still hold and that the diffusive current can be neglected. Following Ref. 16, Eqns. 3 and 4 yield a differential equation for the electric field

$$\mathrm{d}F/\mathrm{d}x = G/F(x) \qquad \text{(A1)}$$

where

$$G = I/(A\mu\varepsilon\theta) \qquad \text{(A2)}$$

with the solution $F(x) = (2Gx)^{1/2}$. The potential is obtained by integrating the electric field along d_i,

$$U = \int_0^{d_i} F(x)\,\mathrm{d}x = \tfrac{2}{3}(2G)^{1/2} d_i^{3/2} \qquad \text{(A3)}$$

and the current is calculated by solving Eqn. A3 for I.

$$I_{\mathrm{SCL}} = \tfrac{9}{8} A\theta\varepsilon\mu U_i^2/d_i^3 \qquad \text{(A4)}$$

Appendix B

Screening by a layer of fixed charge of thickness l_a in front of the emitter. The integral (Eqn. A3) is split into parts that account for the voltage drop, U_1, across the accumulation zone of thickness l_a and for the voltage, U_2, across the hydrocarbon phase.

$$U_i = U_1 + U_2 = \int_0^{l_a} F_1\,\mathrm{d}x + \int_{l_a}^{d_i} F_2\,\mathrm{d}x \qquad \text{(B1)}$$

The first integral is processed as described in Appendix A and the second integral starts with

$$F_2(l_a) = 3U_1/(2l_a) \tag{B2}$$

matching the boundary conditions for F at the interface $x = l_a$ [20].

$$F_2 = (2G((x - l_a)\theta + l_a))^{1/2} \tag{B3}$$

After integration of Eqn. B1 one obtains

$$U_i = \tfrac{2}{3}(2IAd_i^3/(\varepsilon\mu)S_e)^{1/2} \tag{B4}$$

where S_e stands for

$$S_e = \left((l_a/d_i)^{3/2}\theta^{-1/2}(1 - 1/\theta) + (1 + l_a/d_i(\theta^{-1} - 1))^{3/2}\right)^{-2} \tag{B5}$$

A much simpler approximate form of S_e is obtained by assuming that the layer in front of the emitter is the main seat of the space charge. Neglecting the mobile charge in the hydrocarbon phase. The field generated by the layer (Eqn. B2) is approximately equal to the constant field U_i/d_i across the hydrocarbon phase.

$$U_1 = \tfrac{2}{3}U_i l_a/d_i \tag{B6}$$

Substitution of Eqn. B6 into the current-voltage relation for region l

$$I_{SCL} = \tfrac{9}{8}A\theta\varepsilon\mu U_i^2 l_a^{-3} = \tfrac{9}{8}A\varepsilon\mu U_i^2 d_i^{-3}(\tfrac{4}{9}\theta d_i/l_a) \tag{B7}$$

yields the screening factor S_e in the form of

$$S_e = \tfrac{4}{9}\theta d_i/l_a \tag{B8}$$

An analogous screening factor for a layer in front of the collector is calculated in Ref. 18. However, this correction is less important and will be neglected because the integral extends only over the short distance separating it from the collector.

Appendix C

Derivation of Eqn. 9

Abbreviating Eqn. 5 by

$$I_{SCL} = \alpha U^2 \tag{C1}$$

we write

$$I = -\mathrm{d}Q/\mathrm{d}t = -C_i\,\mathrm{d}U/\mathrm{d}t = \alpha U^2 \tag{C2}$$

Integration of Eqn. C2 gives

$$U = C_i/(\alpha t + \beta) \tag{C3}$$

the integration constant β is determined from the boundary condition for $t = 0$ when U_i is applied and ion translocation starts.

$$U_i = C_i/\beta \tag{C4}$$

Substitution of Eqn. C4 into Eqn. C1 yields

$$I = \alpha(\beta U_i/(\alpha t + \beta))^2 \tag{C5}$$

which is rearranged to give

$$I = \alpha U_i^2(t/t_o + 1)^{-2} \tag{C6}$$

by using Eqn. 8

$$\beta/\alpha = d_i^2/(S_e\mu U_i) = t_o \tag{C7}$$

References

1 Andersen, O.S., Feldberg, S., Nakadomari, H., Levy, S. and McLaughlin, S. (1978) Biophys. J. 21, 35–70

2 McLaughlin, S. and Harary, H. (1976) Biochemistry 15, 1941–1948

3 Hall, J.E., Mead, C.A. and Szabo, G. (1973) J. Membrane Biol. 11, 75–97

4 Haydon, D.A. and Hladky, S.P. (1972) Q. Rev. Biophys. 5 187–282

5 Andersen, O.S. and Fuchs, M. (1977) Biophys. J. 17, 796–830

6 Leuchtag, H.R. and Swihart, J.C. (1977) Biophys. J. 17, 27–46

7 Ketterer, B., Neumcke, B. and Läuger, P. (1971) J. Membrane Biol. 5, 225–245

8 Bruner, L.J. (1975) J. Membrane Biol. 22, 125–141

9 Pickar, A.D. and Amos, W.D. (1976) Biochim. Biophys. Acta 455, 36–55

10 Wulf, J., Benz, R. and Pohl, W.G. (1977) Biochim. Biophys. Acta 465, 429–442

11 Hanai, T., Haydon, D.A. and Taylor, J. (1964) Proc. R. Soc. Lond. a 281, 377–391

12 Neumcke, B. and Läuger, P. (1969) Biophys. J. 9, 1160–1170

13 Kozlov, M.M. and Markin, V.S. (1982) Biophysics 27, 652–658

14 Kozlow, M.M., Chernyi, V.V., Sokolov, V.S., Yermakov, Yu. A. and Markin, V.S. (1983) Biophysics 28, 61–67

15 Läuger, P., Benz, R., Stark, G., Bamberg, E., Jordan, P.C., Fahr, A. and Brock, W. (1981) Q. Rev. Biophys. 14, 513–598, p. 556

16 Mark, P. and Helfrich, W. (1961) J. Appl. Phys. 33, 205–215

17 Mott, N.F. and Gurney, R.W. (1948) Electronic Processes in Ionic Crystals, 2nd Edn. (Fowler, R., Mott, N.F., Kapitza, P. and Bullard, E.C., eds.), p. 172, Claredon Press, Oxford

18 Nicolet, M.-A. (1966) J. Appl. Phys. 37, 4224–4235

19 Nicolet, M.A., Rodriguez, V. and Stolla, D. (1968) Surface Sci. 10, 146–164

20 Delannoy, P., Schott, M. and Berrehar, J. (1975) Phys. Stat. Sol. (a) 32, 577–584

21 Bonham, J.S. and Jarvis, D.H. (1977) Austr. J. Chem. 30, 705–720

22 Bonham, J.S. (1978) Austr. J. Chem. 31, 2117–2130

23 De Levie, R. and Seidah, N.G. (1974) J. Membrane Biol. 16, 1–16

24 Gutmann, F. and Lyons, L.E. (1967) in Organic Semiconductors (Hollomon, J.H., Burke, J.E., Chalmers, B., Sproull, R.L. and Tobolsky, A.T., eds.), p. 568, John Wiley and Sons, New York

25 Roberts, G.G. (1974) Transfer and Storage of Energy by Molecules, Vol. 4 (Burnet, G.M., North, M.N. and Sherwood, J.N., eds.), pp. 153–219, John Wiley and Sons, London

26 Feldberg, S.W. and Delgado, A.B. (1978) Biophys. J. 21, 71–86

27 Müller, P., Rudin, D.O., Tien, H.T. and Wescott, W.C. (1962) Nature 194, 979–980

28 Fettiplace, R., Andrews, D.M. and Haydon, D.M. (1971) J. Membrane Biol. 5, 277–296

29 Braun, H.P., Winter, R., Karg, F.H. and Michel-Beyerle, M.E. (1984) Biochim. Biophys. Acta 773, 61–73

30 Szabo, G. (1977) Ann. NY Acad. Sci. 303, 266–280

31 Pickar, A.D. and Benz, R. (1977) J. Membrane Biol. 44, 353–376

32 Benz, R. and Läuger, P. (1977) Biochim. Biophys. Acta 468, 245–258

33 LeBlanc, O.H. Jr. (1969) Biochim. Biophys. Acta 193, 350–360